

# Power System Voltage Stability as Affected by Large-scale PV Penetration

Rakibuzzaman Shah, *Student Member, IEEE*, N.Mithulanthan, *Senior Member, IEEE*, R.C.Bansal, *Senior Member, IEEE*, K.Y.Lee, *Fellow, IEEE* and A.Lomi, *Member, IEEE*

**Abstract--** Voltage instability is considered as one of the main threats to secure operation of power system networks around the world. Grid connected renewable energy-based generation are developing in recent years for many economic and environmental reasons. This type of generation could have significant impact on power system voltage stability given the nature of the primary source of generation and the technology used to energy conversion. This paper examines the impact of large-scale photovoltaic (PV) generation on power system voltage stability. A comprehensive model of large-scale PV generation in IEEE-14 bus test system has been used for the investigation. Various performance measures including critical eigenvalues of Q-V modal matrix, bus participation factor and loading margin (LM), are used to analyze the impact of PV generator on power system static voltage stability.

**Index Terms--** Critical eigenvalue, Q-V modal analysis, realistic loading direction, PV integration, PV reactive power generation.

## I. INTRODUCTION

Utilization of renewable energy comes from the perspective of environmental conservation and fossil fuel shortage. Recent studies suggest that in medium and long terms, photovoltaic (PV) generator will become commercially so attractive that large scale implementation of this type can be seen in many parts of the world [1], [2]. A large-scale PV generation system includes photovoltaic array, DC/AC converter and their controllers. It is a multivariable and non-linear system and its operation depends on environmental conditions. Due to given nature of PV generator, one important issue related to PV is its impact on system stability. Hence, thorough investigation of power system stability with PV is an urgent task as reported in [3], [4].

Among stability issues, voltage instability has been a major concern for power system. Several major power interruptions have been linked to power system voltage instability in recent

past [5], [6]. It has been proved that inadequate reactive power compensation during stressed operating condition can lead to voltage instability. Although large-scale PV is capable of generating reactive power, but, still reactive power generation capability of PV is limited by grid code and normally works very close to the unity power factor (usually operate 0.95 lead lag power factor) [2], [7]. However, the size and position of large PV generator can introduce significant impact on power system voltage stability as the level of PV penetration become a relevant percentage of total installed power. Thus this paper assesses the impact of large-scale PV generation on power system voltage stability.

The case studies are presented in the paper based on IEEE-14 bus test system. Several cases have been considered for the assessment of system voltage stability and these are:

**Case-1:** IEEE-14 bus system with PQ loads has been considered as base case.

**Case-2:** IEEE-14 bus system with PV generator and different power factor operation.

**Case-3:** PV at different locations in IEEE-14 bus system.

**Case-4:** IEEE-14 bus system with different penetrations of PV.

The rest of the paper is organised as follows. Section II provides a brief description of Q-V modal analysis typically used for static voltage stability studies. Modelling of PV generator for stability studied is elaborated in Section III. Section IV is a case study based on IEEE-14 bus test system. Section V gives the relevant conclusion.

## II. METHODOLOGY

Conventional voltage stability assessment takes into account only the steady state analysis (algebraic equations of the system). However, steady state analysis investigates long term voltage stability by providing information like system loading margin, contributing factors to voltage instability, degree of stability [8]. Equation (1) represents the linearized model of the power system at any operating point [9];

$$\begin{bmatrix} \Delta P \\ \Delta Q \end{bmatrix} = \begin{bmatrix} \frac{\partial P}{\partial \theta} & \frac{\partial P}{\partial V} \\ \frac{\partial Q}{\partial \theta} & \frac{\partial Q}{\partial V} \end{bmatrix} \begin{bmatrix} \Delta \theta \\ \Delta V \end{bmatrix} \quad (1)$$

where,  $\Delta P$ ,  $\Delta Q$  are mismatch power vectors.  $\Delta V$ ,  $\Delta \theta$  are unknown voltage magnitude and angle correction vectors. and,

---

Rakibuzzaman Shah, N.Mithulanthan and R.C.Bansal are with the School of Information Technology and Electrical Engineering, the University of Queensland, Australia  
(E-mail: [md.shah@uq.edu.au](mailto:md.shah@uq.edu.au); [mithulan@itee.uq.edu.au](mailto:mithulan@itee.uq.edu.au); [rcbansal@ieee.org](mailto:rcbansal@ieee.org)).

K. Y. Lee is with Department of Electrical and Computer Engineering, Baylor University, Waco, TX 76798-7356, USA  
(E-mail: [Kwang\\_Y\\_Lee@baylor.edu](mailto:Kwang_Y_Lee@baylor.edu)).

A.Lomi is with the Department of Electrical Engineering, INstutut Teknologi Nasional, Malang, Indonesia ( E-mail: [Abraham@itn.ac.id](mailto:Abraham@itn.ac.id)).

$$\begin{bmatrix} \frac{\partial P}{\partial \theta} & \frac{\partial P}{\partial V} \\ \frac{\partial Q}{\partial \theta} & \frac{\partial Q}{\partial V} \\ \frac{\partial Q}{\partial \theta} & \frac{\partial Q}{\partial V} \end{bmatrix} \quad (2)$$

is the Jacobian matrix of real and reactive power flow equations, which is known as standard power flow Jacobian. For steady state analysis of voltage stability standard power flow Jacobian is used and active power is considered as constant. Thus, from (1) the standard power flow equation becomes

$$\begin{bmatrix} 0 \\ \Delta Q \end{bmatrix} = \begin{bmatrix} \frac{\partial P}{\partial \theta} & \frac{\partial P}{\partial V} \\ \frac{\partial Q}{\partial \theta} & \frac{\partial Q}{\partial V} \\ \frac{\partial Q}{\partial \theta} & \frac{\partial Q}{\partial V} \end{bmatrix} \begin{bmatrix} \Delta \theta \\ \Delta V \end{bmatrix} \quad (3)$$

#### A. Q-V Modal Analysis

From (3) the following equation for modal voltage and small reactive power change can be derived as

$$\Delta Q = J_R \Delta V \quad (4)$$

where,  $\Delta Q$  is small change of reactive power,  $\Delta V$  is small change of bus voltage and  $J_R$ , known as power flow reduced Jacobian matrix, can be expressed as follows:

$$J_R = \left| J_{QV} - J_{Q\theta} J_{P\theta}^{-1} J_{PV} \right| \quad (5)$$

From  $J_R$  matrix following expression can be obtained,

$$J_R = \xi_{nnn} \Lambda_{nnn} \eta_{nnn} \quad (6)$$

where,  $\xi$  = matrix of right eigenvectors corresponding to all eigenvalues of the system ( $nnn$ ),  $\Lambda$  = diagonal matrix of system eigenvalues ( $nnn$ ) and  $\eta$  = matrix of left eigenvectors corresponding to all eigenvalues of the system ( $nnn$ ). Here,  $n$  is the number of buses. By using (6) expression for modal voltage and modal reactive power variations corresponding to  $i^{th}$  eigenvalue can be obtained,

$$v_i = \lambda_i^{-1} q_i \quad (7)$$

where,  $v_i$  = modal voltage variation and  $q_i$  = modal reactive power variation,  $\lambda_i$  = eigenvalue of  $i^{th}$  mode obtained from  $J_R$  system matrix.

Magnitude and sign of the eigenvalues of Q-V modal matrix provide the information about system static voltage stability. As the system becomes stressed, one of the eigenvalues of  $J_R$  becomes smaller and the modal voltage becomes weaker. If the magnitude of the eigenvalue is equal to zero, the corresponding modal voltage could be assumed to be at the point of collapse. A system is called as voltage stable if all the eigenvalues of  $J_R$  system matrix are positive, if any of the eigenvalue is negative, the system is unstable [9], [10].

#### B. Bus Participation

The left and right eigenvectors corresponding to the smallest eigenvalue (critical mode) of the system can confer information regarding the mechanism of voltage instability, by identifying the element participating in the corresponding mode. The bus participation factor measuring the participation of the  $k^{th}$  bus to the  $i^{th}$  mode can be given as

$$P_{ki} = \xi_{ki} \eta_{ik} \quad (8)$$

where,  $P_{ki}$  is the  $k^{th}$  bus participation factor of the  $i^{th}$  eigenvalue,  $\xi_{ki}$  right eigenvector (column vector) for the  $i^{th}$  eigenvalue,  $\eta_{ik}$  left eigenvector (row vector) for the  $i^{th}$  eigenvalue.

Bus participation factors corresponding to the critical modes can predict areas or nodes in the power system susceptible to voltage instability. Buses with large participation factors to the critical mode correspond to the most critical system bus or the weakest bus of the system and the close proximity where the top ranked weak buses are located is known as weak area of the system.

### III. PV GENERATOR MODEL

Photovoltaic generator is based on semiconductor device and solid-state synchronous voltage source converter that is analogous to a synchronous machine except the rotating part. It generates a balanced set of sinusoidal voltage at fundamental frequency with rapidly controllable amplitude and phase angle. Voltage source converter converts a DC input voltage into AC output voltage and supply active and reactive power to the system. Fig.1 shows the schematic diagram of the grid connected PV generator.

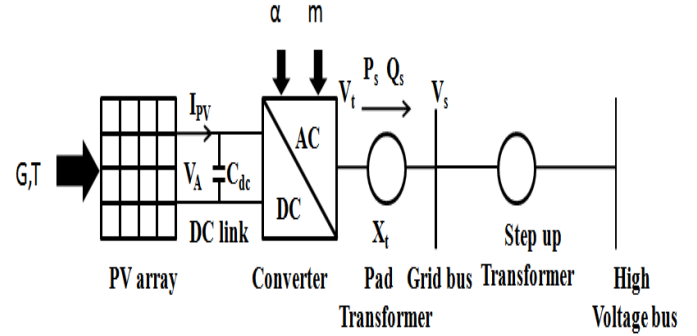


Fig. 1. Schematic diagram of single-stage PV.

#### A. Photovoltaic Array

Solar cell is the basic building block of the photovoltaic array, which is a semiconductor device capable of generating electric power from solar radiation. The performance of the solar cell strongly depends on the radiation and temperature [11], [12]. As the solar cell is only capable of generating very low terminal voltage and output current, so, for the working purposes many cells are connected in series to form higher voltage across the terminal and connected in parallel to form a module. For large scale operation of PV generator, modules are connected in series and parallel to form array. The array output current equation can be derived from basic solar cell output current equation and can be represented as

$$I_{PV} = I_{SCA}(G) - N_P \times I_0 \left[ e^{\frac{(V_A + I_{PV} R_s)q}{nN_S kT}} - 1 \right] \quad (9)$$

where,  $I_{PV}$  = array current (A),  $V_A$  = array voltage (V),  $q$  = electron charge ( $1.6 \times 10^{-19} C$ ),  $k$  = Boltzmann's constant ( $1.38 \times 10^{-19}$ ),  $n$  = ideal factor,  $T$  = ambient temperature,  $I_0$  = reverse saturation current (A),  $R_s$  = array series resistance ( $\Omega$ ),  $I_{SCA}(G)$  =  $N_P I_{SC}(G)$ ,  $N_S = N_{CS} N_{SM}$ ,  $N_P = N_{SP}$ ,  $N_{SM}$  and  $N_{SP}$  represent the number of modules connected in series and parallel in the photovoltaic array, respectively,  $N_{CS}$  = number

of series connected cells in a module,  $I_{SC}$  = cell short circuit current (A) and  $G$  = solar insolation at any instant ( $\text{W/m}^2$ ).

Temperature dependency of reverse saturation current of the cell can be expressed as follows,

$$I_0 = I_r \left[ \frac{T_c}{T_r} \right]^3 \exp\left[\frac{qE_G}{nk}\left(\frac{1}{T_r} - \frac{1}{T_c}\right)\right] \quad (10)$$

where,  $I_r$  = reverse saturation current at standard temperature (A),  $T_c$  = operating temperature (Kelvin),  $T_r$  = reference temperature at standard test condition (Kelvin),  $E_G$  = Energy band gap of solar cell at operating temperature (V).

Temperature and radiation sensitiveness of the solar cell photocurrent can be expressed as follows:

$$I_{SC} = [I_{ph} + \alpha(T_c - T_r)G] \quad (11)$$

where,  $I_{ph}$  = photocurrent at standard condition (A),  $\alpha$  = cell temperature coefficient for short circuit current and  $G$  = solar insolation ( $\text{W/m}^2$ ).

Now, the DC output power of the system can be represented by the following equations,

$$P_{dc} = V_A I_{PV} \quad (12)$$

where,  $V_A$  = PV array terminal voltage, and  $I_{PV}$  = PV array output current.

### B. Power Conditioning Device

Power electronic devices are used for the efficient interfacing between PV array and grid. All the system dynamics of PV generator are related to power conditioning unit [13]. The state variables related to converters and their controllers are

$$[x] = [V_{dc} \ I_d \ I_q \ m \ \alpha] \quad (13)$$

where,  $V_{dc}$  = DC link capacitor voltage,  $I_d$  and  $I_q$  represent dq current components of the voltage source inverter,  $m$  = voltage source converter modulation index, and  $\delta$  = phase angle control of the inverter.

DC power generated from the PV array is considered to be the real power injected in the network. Real and reactive power generation of the system is controlled by voltage source converter. For proper analysis, three-phase inverter terminal voltage is converted into d-q axis voltage component (Park's voltages). Park's voltages are related to the PV array terminal voltage by the following relationship [14]:

$$\begin{cases} V_d = \frac{\sqrt{3}mV_A}{2\sqrt{2}} \cos \delta \\ V_q = -\frac{\sqrt{3}mV_A}{2\sqrt{2}} \sin \delta \end{cases} \quad (14)$$

where,  $m$  is modulation index (0,1),  $\delta$  is the phase angle ( $\pm\pi/2, 0$ ) and  $V_A$  represents PV array terminal voltage.

Let us assume that the DC power generated by the PV array is delivered to the network, then

$$P_{dc} = P_{ac} = \frac{0.6128 m V_A V_s \sin \delta}{X_t} \quad (15)$$

and, the reactive power equation of the PV generator can be represented as

$$Q_{ac} = \frac{0.6128 m V_A \cos \delta}{X_t} - \frac{V_s}{X_t} \quad (16)$$

where,  $V_s$  = grid bus voltage (V), and  $X_t$  = impedance between inverter terminal and grid bus ( $\Omega$ ).

## IV. SIMULATION RESULTS

Single line diagram of IEEE-14 bus test system which is used for the study is depicted in Fig. 2. In the system, there are five synchronous generators among which three of them are synchronous compensators. There are twenty branches and fourteen buses with eleven loads totalling 362.5 MW and 108.5 MVar. A 10 MW<sub>P</sub> [MW peak] size of PV generator has been considered; while for the investigation of the penetration effect of the PV generator on static voltage stability, PV generator size was increased by 10 MW<sub>P</sub> step size. Static data of PV generator for static voltage stability are taken from [15]. Results included in this paper were obtained using MATLAB and MATLAB based power system analysis software known as PSAT [16].

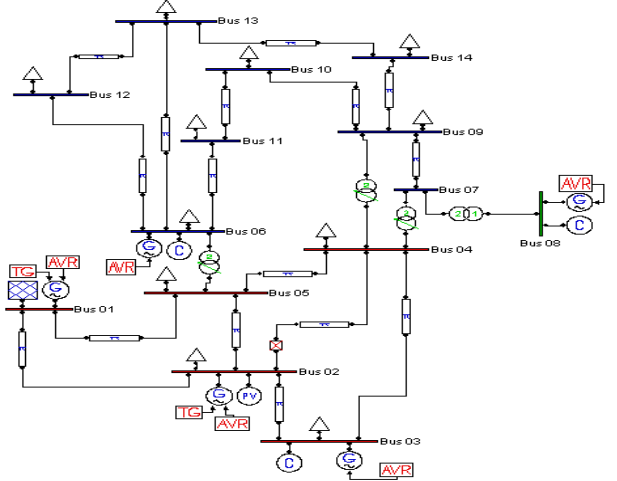


Fig. 2. Single line diagram of IEEE-14 bus system.

### A. Effect of PV Generator

First, Q-V modal analysis has been performed for the base case and then for system with PV. Table I illustrates the three lowest eigenvalues at the base case. The critical eigenvalue of the system at the base case is **2.4855**, which implies system is voltage stable and the saddle-node bifurcation point is not yet reached.

TABLE I  
THREE LOWEST EIGENVALUES AT THE BASE CASE

Lowest eigenvalues	
Mode	Eigenvalue
6	2.4855
7	5.4293
8	7.4796

Fig. 3 illustrates the participation of different buses on the critical eigenvalue. From the figure it is clear that bus 14 is the most contributing bus in this mode, which implies the weakest bus of the system is bus 14. The weak area of the system is identified as the area which consists of buses 14, 11, 9 and 10, as buses 11, 9 and 10 are the weak buses next to bus 14.

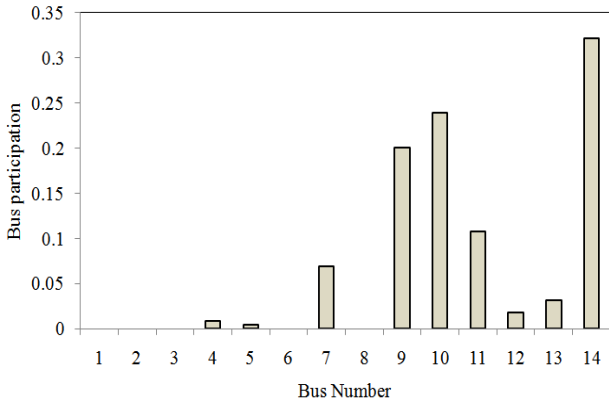


Fig. 3. Participation of system buses on the critical eigenvalue.

In order to see the impact, a PV generator of  $10 \text{ MW}_p$  is installed at the weak area which consists of buses 14, 10, 9 and 11. PV generator is installed at the midpoint of the line in between bus 14 and 9. Table II shows the critical eigenvalues of the system with PV installed in the line between bus 14 and 9. From the table, it is clear that the degree of system voltage stability has been increased after addition of a PV generator to the weak area of the system. The magnitude of the lowest eigenvalue which is indicative of the degree of voltage stability has increased from **2.4855** to **3.6155**. In this case, the PV generator is operating at 0.85 lead-lag power factor.

TABLE II  
THREE LOWEST EIGENVALUES OF THE SYSTEM WITH PV

Lowest eigenvalues	
Mode	Eigenvalue
3	3.6155
5	10.033
8	5.9246

Now, a PV generator has been installed at bus 14 and different power factor operation of the PV generator has been considered. Fig. 4 depicts the effect of different power factor operation of the PV generator on the critical eigenvalue of the Q-V modal matrix.

From Fig. 4 it can be observed that PV integration to the system can increase the degree of voltage stability of the system. Here the power factor is varied from 0.7 (both leading and lagging) to unity. Different power factor operation of PV has significant impact on critical mode as expected, as with the varying power factor the PV generator is dispatching reactive power as well. When the PV generator operates at 0.70 lead-lag power factor, the degree of stability is high among others.

#### B. Effect of PV Location

Integration of PV generator to the grid depends on various factors like solar radiation; land availability, transmission line right-of-way, etc. So, it may not be possible to integrate the PV generator at the weakest bus or the weak area of the system. However, the loading of the system is not constant at all time. Therefore, the effect of load increase and PV location on system voltage stability has been analyzed next.

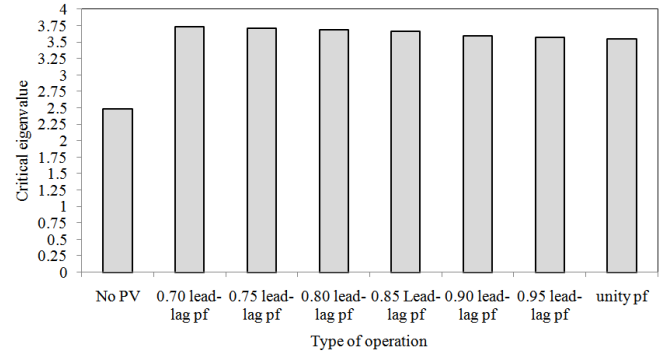


Fig. 4. Comparison of system critical eigenvalues at different operation scenarios.

But, it is difficult to predict loading pattern of the system as it is very complex. In conventional voltage stability analysis the load of each bus is increased at the same rate, as mentioned for conventional loading direction in this paper. But in reality load at the different bus can be changed in different direction, at specific time load of some buses may increase while load in other buses remain unchanged or decreased. For this study we have considered both the conventional loading direction and realistic loading direction proposed in the literature [5] to find the loading margin of the system with PV generator. For realistic load direction, IEEE-14 bus system is split into two areas, namely area-1 and area-2. Buses 1-3, 5 and 6 are in area-1 and buses 4, 7-14 are in area-2. Table III illustrates the percentage of load increase and the area factor for realistic loading direction. PV has been placed at different system buses based on bus weakness. For this analysis  $10 \text{ MW}_p$  size of PV generator and 0.95 lead-lag power factor operation of PV is considered. Fig. 5 shows the system loading margin for two different loading directions and PV generator location on P-V curve. From the figure it is clear that PV location and loading direction has significant impact on loading margin. System with PV generator at bus 12 (conventional loading direction) has less loading margin than system without PV (realistic loading direction).

TABLE III  
THE PERCENT OF LOAD INCREASE AND AREA FACTOR FOR REALISTIC LOADING DIRECTION

Area	% load change	Area factor
1	20.00	0.2944
2	80.00	1.0000

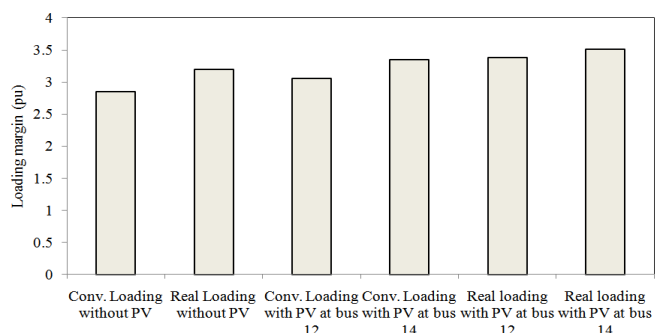


Fig. 5. Loading margins of IEEE-14 bus test system for different loading directions (with and without PV).

Table IV illustrates the effect of PV location on the system critical eigenvalue for normal and N-1 contingency. For this analysis 0.95 lead-lag power factor operation of PV is considered and fault on line 1-5 is considered for N-1 contingency analysis as the outage of this line has severe effect on system performance. Critical eigenvalue of the system at the base case for this particular N-1 contingency is **2.4436**.

TABLE IV  
IMPACT OF PV LOCATION ON CRITICAL EIGENVALUES

PV location bus	Critical eigenvalues	
	Normal	N-1
12	2.6697	2.4025
13	2.6898	2.6091
14	3.9398	3.6791
10,12	4.5266	4.4966
9,13	6.4356	6.4346
5,14	3.9046	3.8876

From the Table IV it can be observed that in all cases the critical eigenvalue is higher than the case without PV for normal operating condition, while during N-1 contingency PV location at bus 12 reduced the degree of stability then the base case for that particular N-1 contingency. From the table, it is worthwhile to note that in most of the cases scattered PV location improves the degree of voltage stability.

### C. Effect of PV Penetration

The effect of an increased PV penetration on power system voltage stability has been studied in IEEE-14 bus test system. The following scenarios are considered for the analysis,

- PV generator at a single location.
- Scattered PV generator location.

For both single and scattered PV penetration, 10 MW<sub>P</sub> to 40 MW<sub>P</sub> with 10 MW<sub>P</sub> step size has been considered for the analysis.

Fig. 6 shows the effect of single location PV penetration on the degree of system stability. From the figure it can be noted that for all buses increase in penetration does not have the positive impact on the system stability. At some location (e.g., bus 12), penetration of PV does not appear to contribute to the voltage stability of the system, meanwhile other position (Bus 9) has both positive and negative impact on voltage stability with incremental penetration. It can be noted that at bus 9, size up to 20 MWp improves the degree of voltage stability, and beyond 20 MWp the degree of voltage stability has been reduced.

Fig.7 shows the impact of scattered PV penetration on the degree of system stability. For scattered penetration, PV generators are placed in three different ways:

- All PVs are in the weak area of the system.
- All PVs are in the strong area of the system.
- PV penetration both in weak and strong area.

From the figure it can be observed that scattered PV penetration enhances the degree of stability. However, the degree of stability enhancement strongly depends on the location of PV.

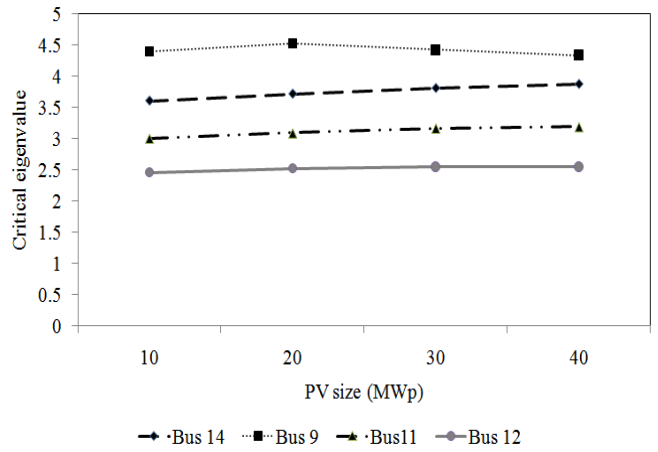


Fig. 6. Effect of PV penetration on the degree of stability for single location.

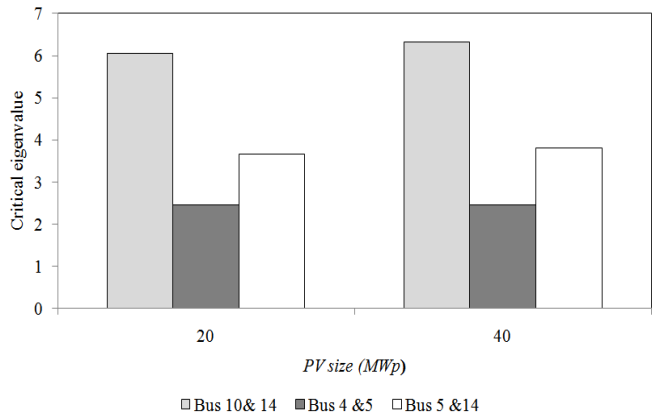


Fig. 7. Effect of PV penetration on the degree of stability for scattered location.

P-V curves of the system with concentrated and scattered PV generator penetration are plotted in Fig. 8. From the figure it can be noted that during higher penetration level, concentrated penetration at bus 14 provides higher loading margin than the scattered penetration at buses 5 and 14 for the same PV size.

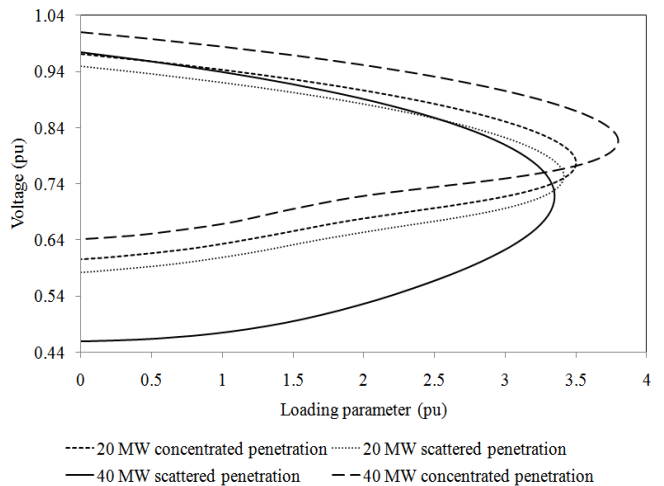


Fig. 8. P-V curve for different PV penetration.

## V. CONCLUSIONS

The paper examines the impact of large-scale PV penetration on static voltage stability of power system. Based on simulation results, it appears that PV location, sizes and the way they are integrated, i.e., as concentrated or scattered, have profound impact on static voltage stability of the system. Moreover, power factor of PV generators also influences the degree of voltage stability as well. Lead-lag power factor operation of PV generator is better compared to unity power factor, while current grid code requirement for distributed generators less than 30 MW strictly stipulate unity power factor operation. The results suggest that there are possibilities for considering some PV generators as ancillary service providers for static voltage stability enhancement of power systems.

## REFERENCES

- [1] M.R.Patel, *Wind and solar power systems: Design, analysis and operation*, CRC press, Boca Raton, USA, 2006.
- [2] M.A.Eltawil and Z.Zhao, "Grid – connected photovoltaic power systems: Technical and potential problems – A review," *Renewable and Sustainable Energy Review*, Vol.14, No.1, pp.112-129, 2010.
- [3] Y.T.Tan, D.S.Kirschen, and N.Jenkins, "A model of PV generation suitable for stability analysis," *IEEE Trans. Energy Conversion*, Vol.19, No.4, pp.748-755, 2004.
- [4] Y.-B. Wang, C.-S.Wu, H.Liao, and H.-H.Xu, " Study on impacts of large-scale photovoltaic power station on power grid voltage profile," in *Third International Conference on Electric Utility Deregulation, Restructuring and Power Technologies*, 2008.
- [5] A.Sode-Yome, N.Mithulananthan, and K.Y.Lee, "Effect of realistic load direction in static voltage stability study," in *IEEE/PES Transmission and Distribution Conference & Exposition: Asia & Pacific*, 2005.
- [6] N.Amajdy and M.Esmaili, " Application of new sensitivity analysis framework for voltage contingency ranking," *IEEE Trans. Power Systems*, Vol.20, No.2, pp. 973-983, 2005.
- [7] X.Xu, Y.Huang, G.He, H.Zhao, and W.Wang, "Modeling of large-scale grid integrated PV station and analysis its impact on grid voltage," in *International Conference on Sustainable Power Generation and supply*, 2009.
- [8] N.Amajdy and M.R.Anvari, "Small disturbance voltage stability evaluation of power systems," in *IEEE/PES Transmission and Distribution Exposition*, 2008.
- [9] P.Kundur, N.J.Balu, and M.G.Lauby, *Power system stability and control*: McGraw – Hill: New York, 1994.
- [10] C.Sharma and M.G.Ganness, "Determination of the applicability of using modal analysis for the prediction of voltage stability," in *IEEE/PES Transmission and Distribution Conference & Exposition: Asia & Pacific*, 2008.
- [11] S.-K.Kim, J.-H.Jeon, C.-H.Cho,J.-B.Ahn, and S.-H.Kwon, "Dynamic Modelling and control of a grid connected hybrid generation system with versatile power transfer," *IEEE Trans. Industrial Electronics*, Vol.55, No.4,pp.1677-1688, 2008.
- [12] M.G.Molina and P.E.Mercado, "Modeling and control of grid – connected photovoltaic energy conversion system used as dispersed generator," in *IEEE/PES Transmission and Distribution Conference & Exposition: Latin America*, 2008.
- [13] S.Alepuz, S. Busquets-Monge, J. Bordonau, J.Gago, D.Gonzalez, and J.Balcells, "Interfacing renewable energy to the utility grid using a three-level inverter," *IEEE Trans. Industrial Electronics*, Vol.53, No.05, pp.1504-1511, 2006.
- [14] F.Delfino, R.Procopio, R.Rossi, and G.Ronda, "Integration of large-size photovoltaic system in to the distribution grids: a p-q chart approach to assess reactive support capability," *IET Renewable Power Generation*, Vol.4, No.4, pp.329-340, 2010.
- [15] K.Clark, N.W.Miller, and R.Walling, "Modeling of GE solar photovoltaic plants for grid studies," General Electric International .Inc, Schenectady, NY 12345, USA, Sep. 9, 2009.
- [16] F.Milano, "PSAT, MATLAB – based power system analysis toolbox, documentation for version 2.00," Mar 24, 2007.